Pergamon

SCIENCE DIRECT

Bioorganic & Medicinal Chemistry 11 (2003) 1835–1849

BIOORGANIC & MEDICINAL CHEMISTRY

Structure-Based Design and Discovery of Novel Inhibitors of Protein Tyrosine Phosphatases

Ping Huang,* John Ramphal, James Wei, Congxin Liang, Bahija Jallal, Gerald McMahon and Cho Tang

SUGEN, Inc., 230 East Grand Ave., South San Francisco, CA 94080, USA

Received 22 July 2002; accepted 27 November 2002

Abstract—Protein tyrosine phosphatases (PTPs) are important in the regulation of signal transduction processes. Certain enzymes of this class are considered as potential therapeutic targets in the treatment of a variety of diseases such as diabetes, inflammation, and cancer. However, many PTP inhibitors identified to date are peptide-based and contain a highly charged phosphate-mimicking component. These compounds usually lack membrane permeability and this limits their utility in the inhibition of intracellular phosphatases. In the present study, we have used structure-based design and modeling techniques to explore catalytic-site directed, reversible inhibitors of PTPs. Employing a non-charged phosphate mimic and non-peptidyl structural components, we have successfully designed and synthesized a novel series of trifluoromethyl sulfonyl and trifluoromethyl sulfonamido compounds as PTP inhibitors. This is the first time that an uncharged phosphate mimic is reported in the literature for general, reversible, and substrate-competitive inhibition of PTPs. It is an important discovery because the finding may provide a paradigm for the development of phosphatase inhibitors that enter cells and modify signal transduction.

Introduction

Protein tyrosine phosphatases (PTPs) constitute a family of receptor-like and cytoplasmic enzymes that catalyze the dephosphorylation of phosphotyrosine residues in protein substrates. PTPs together with protein tyrosine kinases (PTKs) play critical roles in regulating intracellular signal transduction pathways responsible for controlling cell growth, differentiation, motility, and metabolism. Numerous studies have demonstrated the importance of PTPs in physiological processes and that modulation of their enzymatic activity may constitute a therapeutic approach for the treatment of cancer, diabetes, and certain immunologic disorders.[1–3] Several reviews have summarized the current understanding of the biological function, structural characteristics, and biochemical mechanisms of catalysis of PTPs and their roles in signal transduction.[2–5] Importantly, a study with PTP1B knockout mice[6] has demonstrated that loss of PTP1B activity resulted in an enhancement of the insulin sensitivity and resistance to weight gain. This finding suggests that PTP1B inhibitors may be useful for the treatment of Type 2 diabetes and obesity.

During the last several years, a significant number of crystallographic studies of PTPs have been reported.[7–34] These include the tyrosine-specific phosphatases PTP1B,[7–16] Yersinia PTP,[17–19] PTPα,[20] PTPMu,[21] LAR,[22] SHP-2,[23] SHP-1,[24] the dual-specificity phosphatases VHR,[25] Cdc25A,[26] Cdc25B,[27] MAPK phosphatase,[28] and the low-molecular-weight (LMW) phosphatases.[29–34] These crystallographic investigations have provided a wealth of structural information and laid the groundwork for structure-based design of PTP inhibitors. There is a growing interest in the field of PTP inhibitor development and considerable progress has been made (see reviews in 35–37 and references therein). Selective, active site-directed PTP inhibitors have been reported along with a variety of non-hydrolyzable phosphate mimics such as phosphonic acid derivatives,[9,38-43] malonic acid derivatives,[44–48] sulfonic acid,[49,50] tetrazole,[49] cinnamic acid,[51,52] and oxamic acid.[13,14] These phosphate mimics may be incorporated into different frameworks in the design of PTP inhibitors.

*Corresponding author. Tel.: +1-650-837-3422; URL address for SUGEN web site: http://www.sugen.com; e-mail: ping-huang@sugen.com

0968-0896/03/$ - see front matter © 2003 Elsevier Science Ltd. All rights reserved.
doi:10.1016/S0968-0896(03)00039-7

The identification[10] of a second aryl phosphate-binding site adjacent to the active site further provided a paradigm for the design of tight-binding PTP1B inhibitors that can span both sites. Employing the second aryl phosphate-binding site, a tandem pTyr-containing IR peptide substrate of PTP1B was identified with significantly increased affinity.[15] Furthermore, a set of aryl bis-phosphonate based compounds were designed to occupy concurrently the active site and the accessory phosphate site in PTP1B which indeed demonstrated potent inhibitory activity.[53] Efforts to identify new chemical templates of PTP1B inhibitors using high-throughput chemical library screens followed by medicinal chemistry study were reported to develop potent and selective PTP1B inhibitors that were orally active in vivo as antidiabetic agents.[54–56] A similar approach was reported that led to the finding of CD45 inhibitors with cellular activity against T-cell proliferation.[57] In addition, a structure-based computer screening study was reported[58] to identify several interesting small-molecule inhibitors of PTP1B from commercially available chemical databases.

However, many PTP inhibitors known to date are either peptide-based or contain a multi-charged phosphate-mimicking component. Peptidyl compounds are susceptible to proteolytic degradation, and highly charged molecules often exhibit poor cellular uptake. It may thus be necessary to consider non-charged phosphate mimic as well as non-peptidyl scaffold in the development of orally bioavailable PTP inhibitors that can effectively enter cells and modify signal transduction. In the present study, we have used structure-based design and modeling techniques to explore catalytic-site directed, reversible inhibitors of PTPs. Employing a non-charged phosphate mimic and non-peptidyl chemical scaffold, we have successfully designed and synthesized a novel series of trifluoromethyl sulfonyl and trifluoromethyl sulfonamido (TFMS) compounds as PTP inhibitors. The finding of TFMS as a non-charged phosphate mimic is an important discovery. To our knowledge, this is the first time that an uncharged phosphate mimic is reported in the literature for general, reversible, and substrate-competitive inhibition of PTPs.

Insights from Crystal Structures

Crystallographic studies of protein tyrosine phosphatases[7–34] have revealed a highly similar active-site structure. The signature motif $CX_5R(S/T)$ in the tyrosine phosphatases forms a remarkably similar phosphate-binding site with an unusual loop conformation that directs seven sequential main chain NHs toward the phosphate-binding site. These backbone NH groups and the side chain of Arg stabilize the interaction of the phosphoryl group in phosphotyrosine (pTyr) with the active site through a number of hydrogen bonds. In common to all PTPs, the signature motif lies on a loop between a β strand and a helix, located within a crevice on the molecular surface. The phosphate-binding cradle is about 9 Å deep in the tyrosine-specific PTPs. The binding of a substrate or an inhibitor may induce a conformational change of the WpD loop,[8,18] resulting in a closure of the loop and a translocation of the general acid Asp in this loop into the catalytic site.

The crystal structure[8] of PTP1B in complex with a high-affinity substrate (DADEpYL-NH_2) demonstrated that significant ligand–protein interactions occured outside the catalytic site. While the 3-D structure within the catalytic site is highly conserved in PTPs, the surface loops near the catalytic site have some diversity. These results suggest that potent and selective PTP inhibitors could be developed if they favor interactions with not only the catalytic site but also the surface loops in its immediate surroundings, thereby enhancing both affinity and selectivity. Furthermore, the crystallographic study of PTP1B in complex with bis-(*para*-phosphophenyl) methane (BPPM), a synthetic low-molecular-weight non-peptidyl substrate, identified a second aryl phosphate-binding site in PTP1B.[10] This is a low-affinity, non-catalytic binding site adjacent to the active site, with Arg24 and Arg254 forming important interactions with a phosphoryl group in BPPM. The finding of the second pY-binding site indicated that high-affinity inhibitors or substrates of PTP1B could be developed by using appropriate molecular scaffolds that span both the active site and the adjacent, non-catalytic site.

Results and Discussion

Structure-based design and initial lead identification

The objective of our PTP inhibitor program was to identify a novel series of catalytic site-directed, general, and reversible inhibitors of PTPs employing non-charged phosphate mimic and non-peptidyl structure. From the structural insights revealed by the X-ray crystallographic investigations discussed above, it was anticipated that a PTP inhibitor required: (1) a phosphate-mimicking component that replaces or mimics the phosphoryl group in pTyr, and interacts with the PTP signature motif; (2) an aromatic ring that fills the catalytic pocket in a manner reminiscent of the aryl ring in pTyr; and (3) additional structural components that extend beyond the catalytic pocket and interact with the enzyme surface for higher affinity and potential selectivity. With these considerations, our design focused on the search for molecules containing not only a pTyr mimic but also appropriate components for interactions outside the active site.

At the early stage of our study in 1997, only a few published X-ray crystal structures of PTPs, including PTP1B[7,8,10] and Yersinia PTP,[17–19] were available. The co-crystal structure[8] of PTP1B in complex with a high-affinity hexapeptide substrate (DADEpYL-NH_2) was thus selected as a starting point for the modeling studies. Using the de novo design strategy, a search for small molecular fragments that were complementary to the active site in PTP1B was performed via LUDI, a module for de novo ligand design within the program

Insight II.[59] Among the molecular fragments obtained, interestingly, several were aryl sulfonic acids. By its chemical nature, benzene sulfonic acid was considered an acceptable pTyr surrogate. However, the negative charge was thought to be unfavorable for cellular uptake. In an effort to eliminate the charge while retaining the proton-accepting capability that was required for binding interaction with the PTP signature motif, a replacement of the acidic hydroxyl group (−OH) in sulfonic acid with an electronegative, non-acidic $-CF_3$ moiety was considered to be appropriate in the design, as shown in Figure 1. A calculation of the electrostatic potential charge distribution in the trifluoromethylsulfonyl moiety indicated that its surface was partially negatively charged (−0.72 *e* on each oxygen; −0.32 *e* on each fluorine) and would thus be capable of proton-accepting. This resulted in trifluoromethylsulfonyl (TFMS) benzene as a pTyr surrogate. A docking of TFMS-benzene to the catalytic site of PTP1B was subsequently performed using Flexidock, a flexible docking module within the program Sybyl.[60] The results of docking and comparison with the pTyr in the hexapeptide substrate, which was bound to PTP1B in the co-crystal structure,[8] are illustrated in Figures 2 and 3. Figure 2a shows TFMS-benzene docked in the active site of PTP1B, making a number of hydrogen-bonding interactions with the active site. For a direct comparison, the pTyr moiety in the hexapeptide substrate bound to PTP1B[8] is shown in Figure 2b. While the phosphoryl group (Fig. 2b) forms a total of nine hydrogen bonds with the backbone NHs and the side chain of Arg221 in the PTP signature motif, the SO_2CF_3 group (Fig. 2a) makes eight hydrogen bonds with the active site, including an interaction with the backbone NH of Phe182. Clearly, the SO_2CF_3 moiety (TFMS) is able to achieve most hydrogen-bonding interactions that a phosphoryl group makes with the active site. A superimposition (Fig. 3) of the two structures shown in Figure 2 reveals that a sulfone oxygen in TFMS occupies a region near a phosphate oxygen in the pTyr, while the second sulfone oxygen and a fluorine in TFMS are near the other two phosphate oxygens in the pTyr (with a distance of 1.6 and 1.4 Å, respectively). In Figure 3, for a direct comparison, the hydrogen bonds made between the SO_2CF_3 moiety and the active site are shown in yellow while those between the phosphoryl group and the active site are shown in blue. Two fluorines in the CF_3 moiety form a total of three hydrogen bonds with the signature motif as well as the backbone NH of Phe182 (Fig. 2a). The hydrogen bonds that are formed with fluorine as proton acceptor were not surprising, as they had been seen previously[38,39,49,61] in the aryldifluoromethyl phosphonic acids in which fluorine played an important role in the binding interaction directly. Such an interaction was further evident in the X-ray structure[9] of a small molecule, [1,1-difluoro-1-(2-naphthalenyl)-methyl] phosphonic acid, bound to the catalytic site of PTP1B revealing that one of the two fluorine atoms in the molecule formed a hydrogen bond to the backbone NH of Phe182. Taken together, the docking studies suggested that the SO_2CF_3 moiety (TFMS) was a promising candidate of phosphate mimic since it could effectively replicate the important hydrogen-bonding interactions of the parent phosphate with the catalytic site. The non-charged nature of the SO_2CF_3 moiety was of particular interest, since many known PTP inhibitors lacked membrane permeability due primarily to the presence of a negatively charged phosphate mimic.

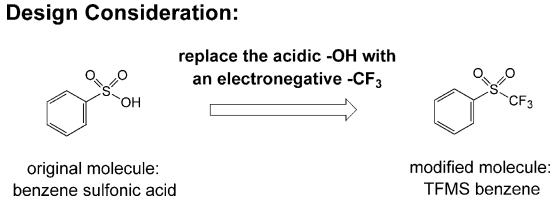

Figure 1. Benzene sulfonic acid was converted to trifluoromethyl sulfonyl (TFMS) benzene in a design study in order to eliminate the negative charge while retaining the proton-accepting capability.

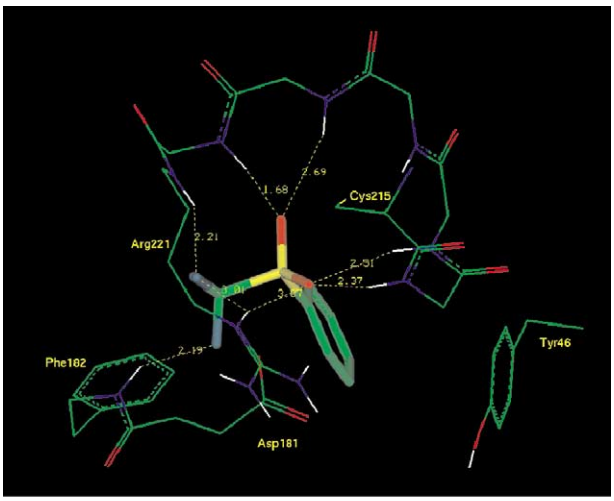

(a)

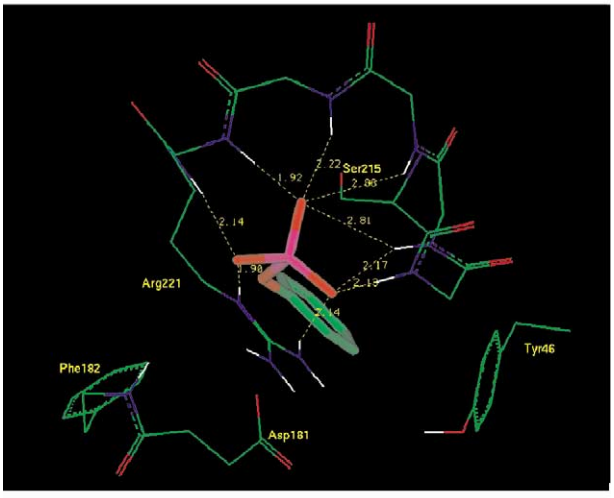

(b)

Figure 2. (a) TFMS-benzene docked in the active site of PTP1B. (b) pTyr in the hexapeptide substrate bound to PTP1B in the co-crystal structure (Brookhaven Data Bank accession code: 1PTU).[8] Only the aryl-phosphate portion of pTyr in the substrate is shown in the figure. Color coding: carbon, green; nitrogen, blue; oxygen, red; hydrogen, white; sulfur, yellow; fluoro, dark green; phosphorus, purple. Non-polar hydrogens are not shown for clarity.

Like phosphotyrosine (pTyr), a TFMS-benzene alone was not expected to exhibit high affinity toward PTPs.

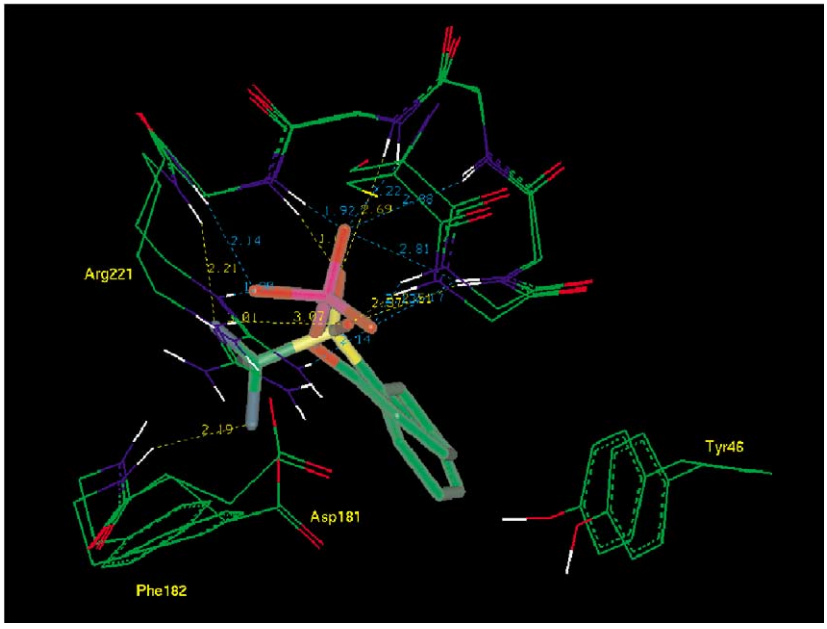

Figure 3. Overlay of the two structures shown in Figure 2 based on a superimposition of the PTP signature motif. The hydrogen-bonding distances between the phosphoryl group and the active site are in light blue, and those between the SO_2CF_3 moiety and the active site are in yellow.

In fact, free pTyr itself was a poor substrate.[62] However, when attached to appropriate peptide templates, the pTyr surrogate-containing molecules became effective PTP inhibitors.[36,62] In order to achieve an inhibitory potency in the primary screen, additional structural components were considered to be necessary in a TFMS-benzene containing molecule. Following a substructure search of commercially available chemical databases such as Available Chemicals Directory (ACD),[63] several compounds containing TFMS-benzene were selected and subjected to docking studies. Among these compounds, bis(4-trifluoromethylsulfonylphenyl) disulfide (**1**, Fig. 4) was determined to be a good candidate. Figure 5 shows this compound docked into the

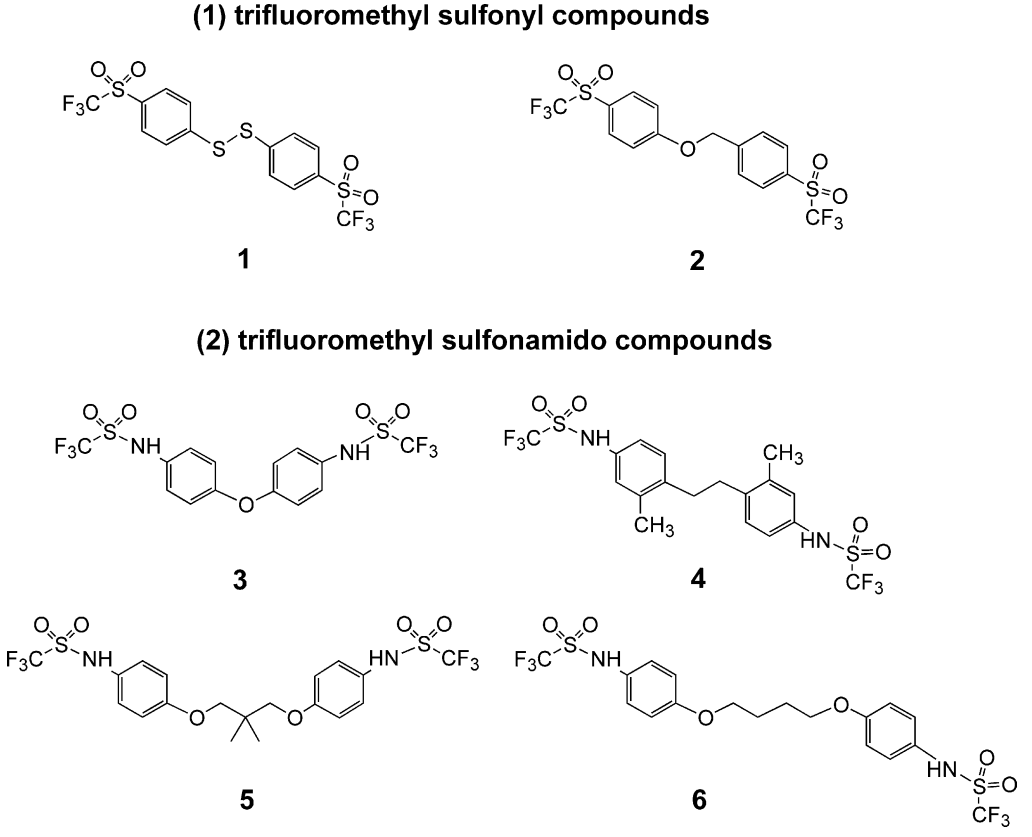

Figure 4. TFMS compounds **1**–**6**.

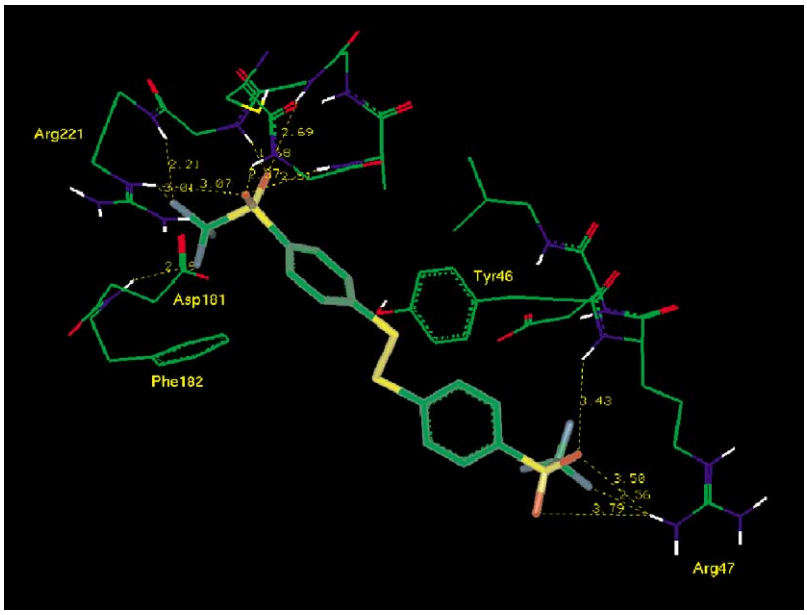

Figure 5. Compound **1** docked in PTP1B. Color coding: carbon, green; nitrogen, blue; oxygen, red; hydrogen, white; sulfur, yellow; fluorine, dark green. Non-polar hydrogens are not shown for clarity.

active site of PTP1B. In addition to the interactions seen before within the active site (Fig. 2a), the proximal half of this molecule extended into the solvent and made interactions with the protein surface. These included the hydrogen-bonding interactions of the second SO_2CF_3 moiety with the guanidinium side chain and the backbone NH of Arg47, as well as the favorable hydrophobic interaction between the second phenyl and Tyr46 (Fig. 5). Indeed, the biochemical screening results were encouraging as shown in Table 1. Compound **1** demonstrated moderate inhibitory activity toward PTP1B and several other phosphatases. A kinetic analysis using pNPP as substrate revealed that this compound was a substrate-competitive inhibitor of PTP1B (Fig. 6). Furthermore, this compound was found to be non-cytotoxic at a concentration of up to 300 μM. This chemical lead strongly suggested that the molecular scaffold could be a good starting point for PTP inhibitor synthesis and analogue exploration.

Analogues of the initial lead

The disulfide bond in compound **1** was expected to be metabolically labile. The initial medicinal chemistry efforts thus focused on the replacement of the disulfide bond with a linkage that could be more stable, as exemplified by **2** in Figure 4. The result that **1** and **2** shared similar activity (Table 1) suggested that the linkage could be diversified while maintaining the TFMS group as essential for inhibitory activity. Furthermore, it was anticipated that a trifluoromethyl sulfonamido group ($-NHSO_2CF_3$) might be able to play a similar role as the trifluoromethyl sulfonyl group ($-SO_2CF_3$) due to their similar chemical nature. Such a change could, however, simplify the synthesis greatly, as discussed later. The screening results indeed supported this hypothesis. As shown in Table 1, the trifluoromethyl sulfonamido compounds **4**–**6** (Fig. 4) demonstrated PTP inhibitory activities that were generally comparable to the trifluoromethyl sulfonyl compounds **1** and **2**. As a result, the concept of TFMS as a phosphate mimic was extended to include both the trifluoromethyl sulfonyl and the trifluoromethyl sulfonamido groups.

The data in Table 1 also revealed that the length of the flexible, linear linker between the two TFMS-benzene moieties did not alter the activity significantly, except

Table 1. Biochemical screening data on PTPs, IC_{50} (μM)

Compd	SHP-2	1B	Epsilon	Meg-2	Sigma	Beta	Mu
1	19	68	24	46	41	23	>100
2	43	56	8.1	62	31	3.5	>100
3	>100	>100	23	>100	>100	>100	76
4	17	35	51	86	41	56	41
5	6.2	45	37	34	12	15	42
6	17	85	48	71	38	7.0	65

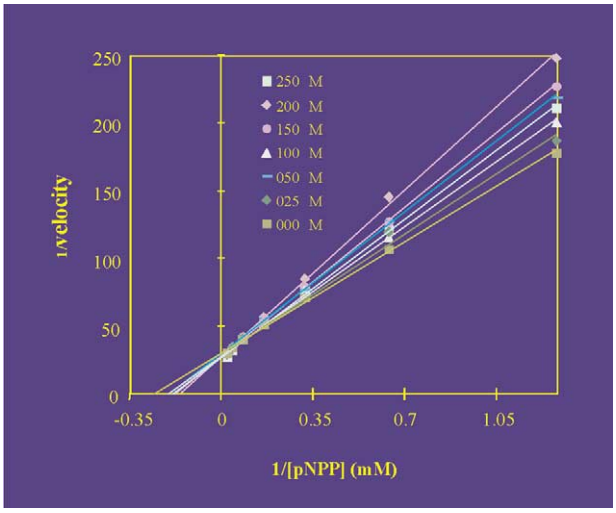

Figure 6. Effect of compound **1** on the hydrolysis of pNPP by PTP1B, suggesting that **1** is a substrate-competitive inhibitor.

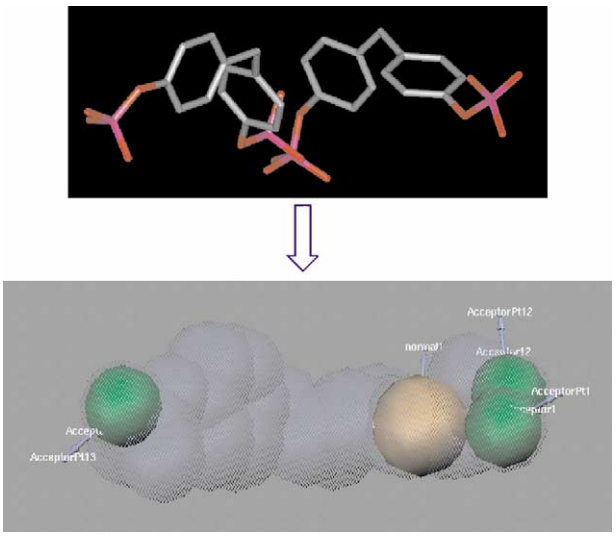

Figure 7. Generation of a 3D pharmacophore using the aryl-phosphate moieties in the two BPPM molecules that were directly involved in the binding interactions with the active site and the non-catalytic site in the PTP1B/C215S-BPPM co-crystal structure (Brookhaven Data Bank accession code: 1AAX).[10] Color coding for BPPMs (top): carbon, gray; oxygen, red; phosphorus, purple. Color coding for the 3D pharmacophore (bottom): proton acceptors, green; aromatic ring, yellow; shape constraint, light blue.

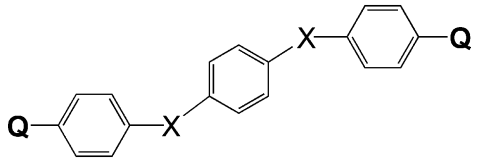

Figure 8. A generic structure that can span both the active site and the non-catalytic pTyr-binding site. Q is a phosphate or phosphate mimic. X is a sp^3 carbon or oxygen.

for compound **3** which contained a one-atom linker and was found to be generally inactive in PTPs. These results were consistent with the assumption that while one of the two TFMS-benzene moieties would interact with the active site, the proximal half of the molecule, extended into the solvent, would be sufficiently flexible to interact with the immediate surroundings outside the catalytic site. Therefore, molecules with various lengths exhibited similar activity. However, a one-atom linker would be too short to achieve these interactions outside the catalytic site, as shown by modeling study.

The crystal structures of PTP1B/C215S-BPPM and PTP1B/C215S-pTyr complexes revealed a second aryl phosphate-binding site in PTP1B.[10] This low-affinity, non-catalytic site is adjacent to the active site, with Arg24 and Arg254 forming important interactions with a phosphoryl group in BPPM or pTyr. This finding provided a new opportunity for developing PTP inhibitors that target the two extended binding sites rather than the catalytic site alone. We incorporated this new finding in our design of TFMS compounds that could occupy both the active site and the non-catalytic site to achieve higher potency. From the aryl-phosphate moieties in the two BPPM molecules that were directly involved in the binding interactions with the active site and the non-catalytic site in the PTP1B/C215S-BPPM co-crystal structure,[10] we generated a 3D pharmacophore (Fig. 7) to search databases for appropriate structures that could span both sites by using modeling software Catalyst.[64] The results suggested that the generic structure shown in Figure 8 was able to occupy both sites simultaneously, in which Q is a phosphate or phosphate mimic, and X is a sp^3 carbon or oxygen. To test this hypothesis, compounds **7** and **8** (Fig. 9) were synthesized. As shown

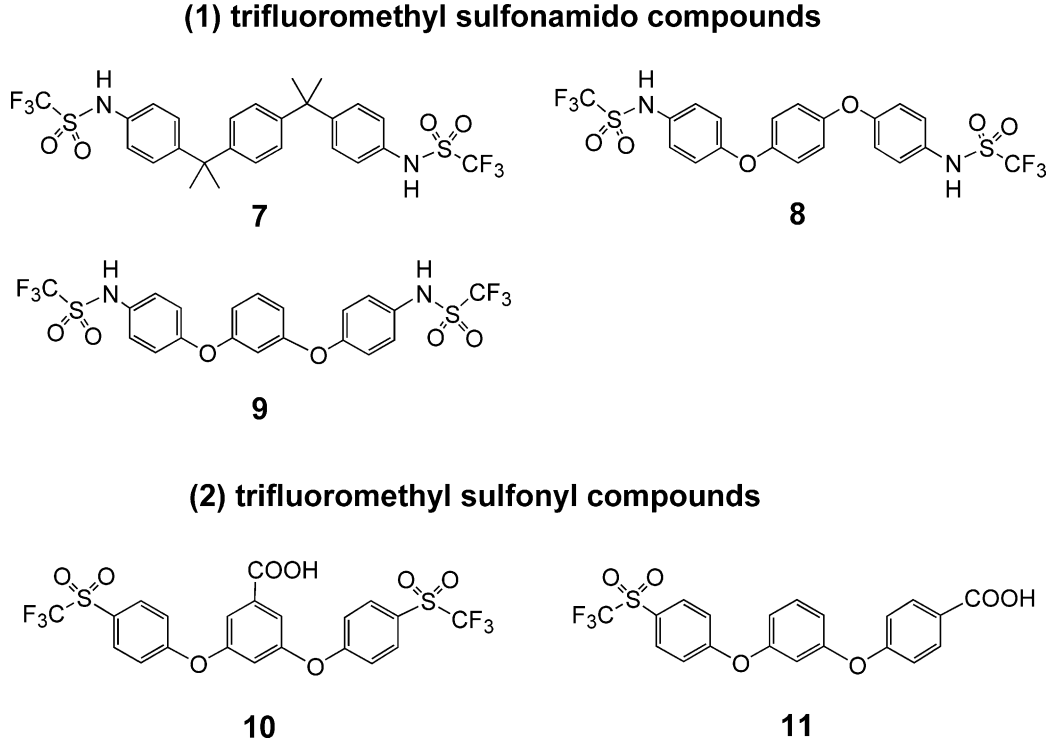

Figure 9. TFMS compounds **7**–**11**.

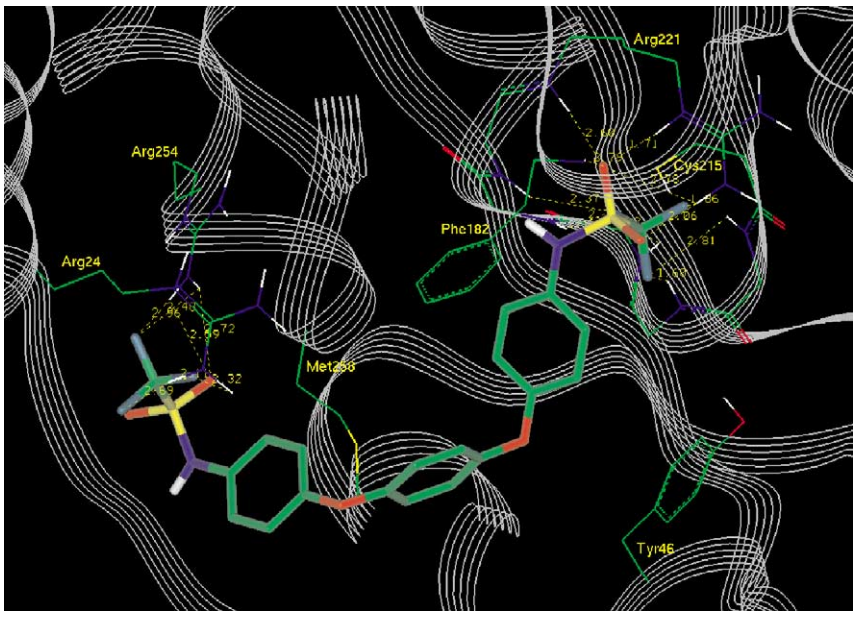

Figure 10. Compound **8** docked in the PTP1B structure,[8] making interactions with both the active site and the non-catalytic site. Color coding: carbon, green; nitrogen, blue; oxygen, red; hydrogen, white; sulfur, yellow; fluorine, dark green; line-ribbon representation of PTP1B backbone, gray. Non-polar hydrogens are not shown for clarity.

in Table 2, both compounds demonstrated significantly increased potency in several PTP biochemical assays including PTP1B when compared with those in Table 1.

Figure 10 illustrates compound **8** docked in the PTP1B structure, making interactions with both the active site and the non-catalytic site. A number of hydrogen bonds were seen in Figure 10 between the SO_2CF_3 moiety and the side chains of Arg24 and Arg254 in the non-catalytic site, while significant interactions within the active site were maintained. A direct comparison of compound **8** with the two BPPM molecules bound to PTP1B[10] is shown in Figure 11. This overlay was made based on a superimposition of the PTP1B structure with **8** docked and that in the PTP1B-BPPM co-crystal structure.[10] Clearly from this figure, the two TFMS-phenyls of **8** are close to the aryl-phosphate moieties of the BPPM molecules interacting with the active site (top) and the non-catalytic site (bottom left) respectively in the crystal structure.[10]

It was noticed in Table 2 that compounds **7** and **8** showed greatly increased potency not only on PTP1B but also on the phosphatases SHP-2 and Mu. Our structure-based sequence alignment study indicated that the residue Arg254 of PTP1B in the non-catalytic site is well conserved in some PTPs. The corresponding residue in PTPα is Arg469, Arg1131 in Mu, Arg498 in SHP-2, Arg494 in SHP-1, and Arg437 in Yersinia PTP. Therefore, the interaction of the second SO_2CF_3 moiety in compounds **7** and **8** with this conserved Arg may explain the increased inhibitory potency towards several PTPs in addition to PTP1B. To directly probe this and explore the importance of the TFMS group in these compounds to their PTP inhibitory activity, a comparison of **8** with compounds **12** and **13** (Fig. 12) was made. As clearly demonstrated in Table 3, removal of one CF_3SO_2 moiety in **8** resulted in a decrease in activity in general when tested on most PTPs (**12**, Table 3), consistent with the loss of interaction with the low-affinity, non-catalytic binding site. Furthermore, removal of

Table 2. Biochemical screening data on PTPs, IC_{50} (μM)

Compd	SHP-2	1B	Epsilon	Meg-2	Sigma	Beta	Mu
7	1.8	2.5	8.4	13	20	6.4	6.7
8	3.4	11	17	39	44	12	4.0
9	2.8	7.7	1.8	59	7.6	27	3.9
10	5.7	6.2	1.8	9.6	7.7	4.5	8.7
11	18	16	0.77	44	22	14	22

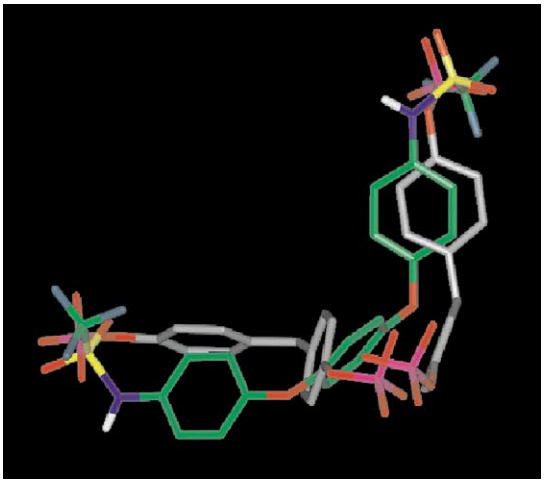

Figure 11. Comparison of **8** with the two BPPM molecules bound to PTP1B in the co-crystal structure (Brookhaven Data Bank accession code: 1AAX).[10] The two TFMS-phenyls of **8** are close to the aryl-phosphate moieties of BPPMs interacting with the active site (top) and the non-catalytic site (bottom left), respectively. Color coding: nitrogen, blue; oxygen, red; hydrogen, white; sulfur, yellow; fluorine, dark green; phosphorus, purple; carbons in **8**, green; carbons in BPPM, gray. Non-polar hydrogens are not shown for clarity.

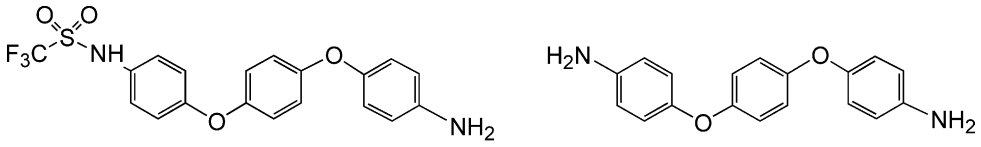

12 **13**

Figure 12. Compounds **12** and **13** were included in a direct comparison with **8**.

both CF_3SO_2 moieties in **8** led to a complete loss of activity on all PTPs (**13**, Table 3). This result provided a strong support to our hypothesis that the TFMS group would be essential for the inhibitory activity, supporting its role as a phosphate mimic. The difference in activity between **8** and **12** was somewhat smaller than expected. It is likely that either the binding of the second TFMS group of **8** to the non-catalytic site was not as strong as predicted, or the aniline portion of **12** picked up some interactions with the protein surface, resulting in higher affinity of **12** than expected.

While compounds **7** and **8** shared a 1,4-di-substituted phenyl linkage (Fig. 9), some analogues with a 1,3-phenyldioxy linker (**9**–**11**) were also explored. From the structural point of view, a 1,3-phenyldioxy linkage would be expected to place the two SO_2CF_3 moieties in the appropriate positions to interact with the active site and the non-catalytic site as well. A superimposition of **10** with the two BPPM molecules that were bound to PTP1B in the co-crystal structure[10] is shown in Figure 13. The position and orientation of the 1,3-phenyldioxy linker in **10** (Fig. 13) were found to be different from those of the 1,4-phenyldioxy linker in **8** (Fig. 11). Both were, however, determined to be appropriate following docking to PTP1B because the linkages were essentially in the solvent-accessible region on the protein surface. Consistent with this result, comparable potencies of compounds **8**–**10** on PTP1B, SHP-2, and Mu were found (Table 2). In addition, Table 2 shows that compound **11**, which contains a carboxyl group in replacement of one TFMS moiety, exhibited moderate inhibitory activity towards most PTPs, suggesting that the common proton-accepting nature of TFMS and the carboxyl group in these compounds may be responsible for the interactions with the non-catalytic site. Nevertheless, compound **11** exhibited good potency and selectivity towards phosphatase Epsilon (Table 2) due to the presence of the carboxyl group. These results revealed the potential of the approach to achieve compounds with potency and selectivity for PTP inhibition. As seen in Tables 1 and 2, both trifluoromethyl sulfonyl and trifluoromethyl sulfonamido analogues were included in the present study. To access the relative effectiveness of the trifluoromethyl sulfonyl and trifluoromethyl sulfonamido groups in binding, direct comparisons of some analogues have been made (data not shown). However, no general trend was observed because the relative effectiveness of the groups in binding appeared to be linker-dependent.

Table 3. A direct comparison of the biochemical screening data [IC_{50} (μM)] to probe the effect of the SO_2CF_3 group

Compd	SHP-2	1B	Epsilon	Meg-2	Sigma	Beta	Mu
8	3.4	11	17	39	44	12	4.0
12	17	28	48	>100	41	23	>100
13	>100	>100	>100	>100	>100	>100	>100

Taken together, the results shown in Table 2 are consistent with the hypothesis that the second TFMS benzene moiety may bind to the non-catalytic pY-binding site. Nevertheless, these results do not eliminate the possibility that this second TFMS moiety bound to other residues on the protein surface such as Arg47 in PTP1B. A recent report[65] of co-crystal structures of PTP1B in complex with inhibitors bearing two phosphotyrosine mimetics revealed that the second or distal phosphonate group extended into the solvent and made water-mediated interactions with Arg47 in PTP1B rather than going to the non-catalytic pY-binding site. Clearly, X-ray co-crystallography studies of PTPs in complex with the TFMS compounds reported herein are necessary to verify the binding mode of these molecules.

Synthesis

The synthesis of the PTP inhibitors was easily accessed in short order. Thus, 4-(trifluoromethylthio)benzyl alcohol was arylated with 4-(trifluoromethylsulfonyl)-chlorobenzene and sodium hydride to afford 4-trifluoromethylthiobenzyl 4-trifluoromethylsulfonylphenyl ether. Subsequent MCPBA oxidation gave the desired

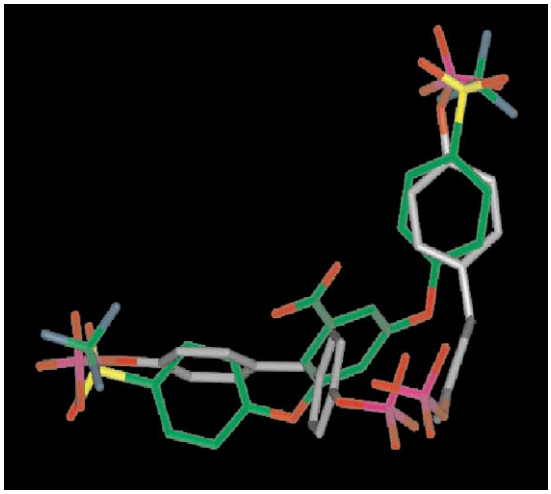

Figure 13. Comparison of **10** with the two BPPM molecules bound to PTP1B in the co-crystal structure (Brookhaven Data Bank accession code: 1AAX).[10] The two TFMS-phenyls of **10** are close to the aryl-phosphate moieties of BPPMs interacting with the active site (top) and the non-catalytic site (bottom left), respectively. Color coding: oxygen, red; sulfur, yellow; fluorine, dark green; phosphorus, purple; carbons in **10**, green; carbons in BPPM, gray. Non-polar hydrogens are not shown for clarity.

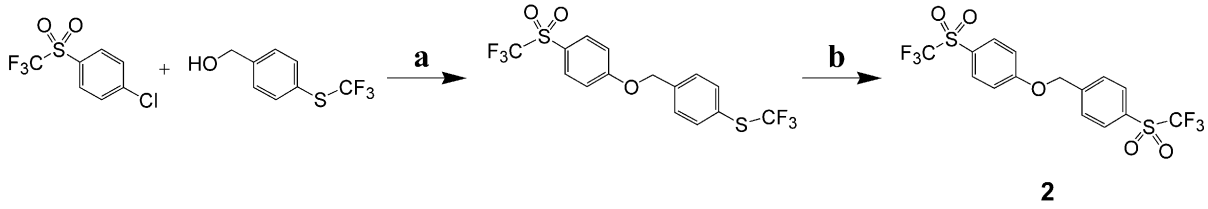

Scheme 1. Synthesis of compound **2**. Reagents: (a) NaH; (b) 3-chloroperbenzoic acid.

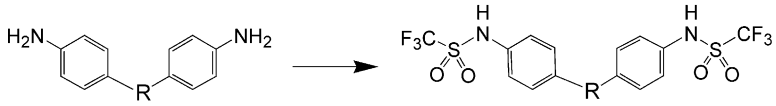

Scheme 2. Synthesis of trifluoromethyl sulfonamido compounds **3–9**. Reagents: $(CF_3SO_2)_2O$, $NaHCO_3$, CH_2Cl_2, room temperature.

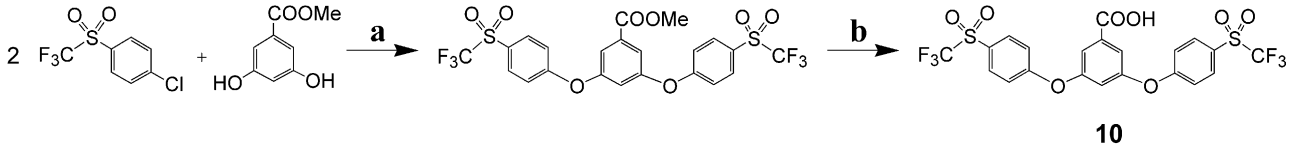

Scheme 3. Synthesis of trifluoromethyl sulfonyl compound **10**. Reagents: (a) K_2CO_3, DMF, 125 °C; (b) KOH, THF, H_2O.

bis trifluoromethylsulfone derivative **2** depicted in Scheme 1. The trifluoromethylsulfonamide derivatives (**3–9**) (Scheme 2) were obtained through the sulfonylation of the corresponding anilines in the presence of triflic anhydride and sodium bicarbonate in dichloromethane under ambient conditions. Finally, bis trifluoromethylsulfone ether **10** was obtained in a similar fashion as 2 (Scheme 3). Methyl 3,5-dihydroxybenzoate was arylated with 4-(trifluoromethylsulfonyl)chlorobenzene under basic conditions (potassium carbonate, DMF, 125 °C) to afford the corresponding bis ether methyl ester. Alkaline hydrolysis resulted in the desired compound **10**.

Conclusion

We described here the rational design and medicinal chemistry studies to explore catalytic-site directed, reversible inhibitors of PTPs. Using the structure-based design and modeling techniques, we have initially identified a lead compound with the trifluoromethyl sulfonyl moiety as a non-charged phosphate mimic. Optimization of this lead was subsequently driven by medicinal chemistry approach together with a design based on modeling study to incorporate molecular scaffolds that are able to span both the active site and the adjacent, non-catalytic site for greater potency. These efforts have successfully led to the discovery of a novel series of trifluoromethyl sulfonyl and trifluoromethyl sulfonamido compounds as PTP inhibitors. This is the first time that an uncharged phosphate mimic is reported in the literature for general, reversible, and substrate-competitive inhibition of PTPs. It is an important discovery because the finding may provide a paradigm for the development of phosphatase inhibitors that could ultimately be therapeutically useful agents.

Experimental

Molecular modeling. All molecular modeling studies were performed using commercially available software packages Sybyl (6.4),[60] Insight II (97.0),[59] and Catalyst (4.5)[64] running on Silicon Graphics Indigo II (R10000) and Octane workstations. For docking studies, the co-crystal structure[8] of PTP1B in complex with a hexapeptide substrate, downloaded from Brookhaven Data Bank (accession code: 1PTU), was used as a starting structure in which the substrate and waters were removed and Ser215 was mutated back to a cysteine residue. The TFMS-phenyl moiety in the docked compounds was initially placed into the active site, and the protein–ligand complex was energy minimized using Tripos force field. Flexible docking was performed using Sybyl6.4/Flexidock. Charges were calculated via the Gasteiger–Huckel method, and the distance-dependent dielectric function with a dielectric constant of 1 was employed. Nonbonded cutoff was set to 8 Å. The movable region of PTP1B included atoms within 6 Å from the docked compound, which was completely flexible. The fitness scoring function was based on a subset of Tripos force field including van der Waals, electrostatic, and torsional terms, in combination with the score for favorable hydrogen-bonding interactions. The best-scored structure obtained by Flexidock was further energy minimized to give the final structure.

Chemistry

Compounds **1** and **13** were purchased from commercial sources and used as received. Compounds **2–12** were synthesized as described below. ^1H NMR spectra were recorded by Acron NMR using a Nicolet NT300 or a Nicolet NT360. ^{13}C NMR spectra were collected on a

Varian INOVA 600 MHz NMR spectrometer. ^{19}F NMR spectra were collected on a Varian Mercury 400 MHz NMR spectrometer. High-resolution mass spectra (HRMS) were obtained on a Voyager-DE STR MALDI/TOF spectrometer (Applied Biosystems). All final products were analyzed for purity by reverse-phase high-performance liquid chromatography (HPLC) and were found to be >90% pure.

4-Trifluoromethylsulfonylbenzyl 4-trifluoromethylsulfonylphenyl ether (2). To a solution of 4-(Trifluoromethylthio)benzyl alcohol (300 mg, 1.44 mmol) in dry THF (6.0 mL) at 0 °C was added sodium hydride (65 mg, 60% dispersion in oil, 1.58 mmol. The resulting mixture was stirred for 15 min followed by addition of 4-(trifluoromethylsulfonyl)chlorobenzene (370 mg, 1.51 mmol). The reaction mixture was warmed to 25 °C and stirring continued for 8 h. The reaction was quenched with H_2O (5 mL) and the resulting solution diluted with EtOAc (200 mL) followed by washing with H_2O (100 mL), brine (100 mL), dried ($MgSO_4$), and concentrated by rotary evaporation to give a cream solid that was purified via silica gel chromatography (hexane–EtOAc, 90:10) to give the intermediate ether as a white solid (400 mg). ^1H NMR (360 MHz, DMSO-d_6) δ 8.06 (d, J = 8.4 Hz, 2H), 7.77 (d, J = 8.4 Hz, 2H), 7.63 (d, J = 8.4 Hz, 2H), 7.43 (d, J = 8.4 Hz, 2H), 5.39 (s, 2H, OCH_2).

To a solution of 4-trifluoromethylthiobenzyl 4-trifluoromethylsulfonylphenyl ether (66 mg, 0.16 mmol) in CH_2Cl_2 (6 mL) at 0 °C was added 3-chloroperbenzoic acid (100 mg, 57–86%, 0.58 mmol). The resulting mixture was stirred for 1 h before warming to 25 °C and stirring continued for 3 h. The reaction was quenched with $NaHCO_3$ (50 mL) and the resulting solution diluted with EtOAc (200 mL) followed by washing with H_2O (2×100 mL), brine (100 mL), dried ($MgSO_4$), and concentrated by rotary evaporation to give a cream solid that was purified via silica gel chromatography (hexane–EtOAc, 80:20) to give 4-trifluoromethylsulfonylbenzyl 4-trifluoromethylsulfonylphenyl ether (**2**) as a white solid (53 mg). ^1H NMR (360 MHz, DMSO-d_6) δ 8.20 (d, J = 8.6 Hz, 2H), 8.09 (d, J = 8.6 Hz, 2H), 7.93 (d, J = 8.6 Hz, 2H), 7.45 (d, J = 8.6 Hz, 2H), 5.55 (s, 2H, OCH_2). MS-EI m/z 448 [M^+]. HRMS calcd for $C_{15}H_{10}F_6O_5S_2$ [M – H]$^-$ 446.9796, found 446.9825.

Bis(4-trifluoromethylsulfonamidophenyl) ether (3). To a solution of 4,4′-diaminodiphenyl ether (500 mg, 2.5 mmol) in dry CH_2Cl_2 (8 mL) at 0 °C was added sodium bicarbonate (840 mg, 10 mmol) and $(CF_3SO_2)_2O$ (0.84 mL, 5 mmol). The resulting mixture was stirred for 15 min. The reaction mixture was warmed to 25 °C and stirring continued for 18 h. The reaction was quenched with H_2O (100 mL) and the resulting solution diluted with EtOAc (200 mL) followed by washing with brine (100 mL), dried ($MgSO_4$), and concentrated by rotary evaporation to give a cream solid that was purified via silica gel chromatography (hexane–EtOAc, 70:30) to give bis(4-trifluoromethylsulfonamidophenyl) ether, **3,** (893 mg). ^1H NMR (300 MHz, DMSO-d_6) δ 11.7 (br s, 2H, 2×NH), 7.26 (m, 4H), 7.06 (m, 4H). ^{19}F NMR (376.5 MHz, DMSO) δ 75.91 (s, 6F, 2×CF_3). ^{13}C NMR (600 MHz, DMSO-d_6) δ 154.7, 125.5, 125.4, 119.5, 119.3. MS-EI m/z 464 [M^+]. HRMS calcd for $C_{14}H_{10}F_6N_2O_5S_2$ [M– H]$^-$ 462.9857, found 462.9839.

1,2 - Bis(2 - methyl - 4 - trifluoromethylsulfonamidophenyl)-ethane (4). To a solution of 4,4′-diamino-2,2′dimethylbibenzyl (500 mg, 2.08 mmol) in dry CH_2Cl_2 (7 mL) at 0 °C was added sodium bicarbonate (700 mg, 8.32 mmol) and $(CF_3SO_2)_2O$ (0.77 mL, 4.6 mmol). The resulting mixture was stirred for 15 min. The reaction mixture was warmed to 25 °C and stirring continued for 18 h. The reaction was quenched with H_2O (100 mL) and the resulting solution diluted with EtOAc (200 mL) followed by washing with brine (100 mL), dried ($MgSO_4$), and concentrated by rotary evaporation to give a cream solid that was purified via silica gel chromatography (hexane–EtOAc, 70:30) to give 1,2-bis(2-methyl-4-trifluoromethylsulfonamidophenyl) ethane, **4**, (754 mg). ^1H NMR (300 MHz, DMSO-d_6) δ 11.61 (s, br, 2H, 2×NH), 7.14 (d, J = 7.5 Hz, 2H), 6.99 (m, 4H), 2.75 (s, 4H, 2×CH_2), 2.21 (s, 6H, 2× CH_3). ^{19}F NMR (376.5 MHz, DMSO) δ 75.87 (s, 6F, 2×CF_3). ^{13}C NMR (600 MHz, DMSO-d_6) δ 156.3, 137.1, 132.4, 129.8, 124.6, 120.8, 118.7, 32.6, 18.8. MS-EI m/z 504 [M^+]. HRMS calcd for $C_{18}H_{18}F_6N_2O_4S_2$ [M – H]$^-$ 503.0534, found 503.0521.

1,3 - Bis(4 - trifluoromethylsulfonamidophenoxy) - 2,2 - dimethylpropane (5). To a solution of neopentyl glycol bis(4-aminophenyl) ether (500 mg, 1.75 mmol) in dry CH_2Cl_2 (7 mL) at 0 °C was added sodium bicarbonate (590 mg, 7 mmol) and $(CF_3SO_2)_2O$ (0.65 mL, 3.9 mmol). The resulting mixture was stirred for 15 min. The reaction mixture was warmed to 25 °C and stirring continued for 18 h. The reaction was quenched with H_2O (100 mL) and the resulting solution diluted with EtOAc (200 mL) followed by washing with brine (100 mL), dried ($MgSO_4$), and concentrated by rotary evaporation to give a cream solid that was purified via silica gel chromatography (hexane–EtOAc, 70:30) to give 1,3-bis(4-trifluoromethylsulfonamidophenoxy)-2,2-dimethylpropane, **5**, (724 mg). ^1H NMR (300 MHz, DMSO-d_6) δ 11.55 (s, br, 2H, 2×NH), 7.13 (d, J = 9.15 Hz, 4H), 6.96 (d, J = 9.15 Hz, 4H), 3.82 (s, 4H, 2×CH_2), 1.07 (s, 6H, 2×CH_3). ^{19}F NMR (376.5 MHz, DMSO) δ 75.74 (s, 6F, 2×CF_3). ^{13}C NMR (600 MHz, DMSO-d_6) δ 156.7, 125.8, 120.8, 116.5, 115.2, 73.1, 35.5, 21.5. MS-EI m/z 550 [M^+]. HRMS calcd for $C_{19}H_{20}F_6N_2O_6S_2$ [M – H]$^-$ 549.0589, found 549.0563.

1,4-Bis(4-trifluoromethylsulfonamidophenoxy)butane (6). To a solution of 4-[4-(4-aminophenoxy)butoxy]aniline (500 mg, 1.84 mmol) in dry CH_2Cl_2 (7 mL) at 0 °C was added sodium bicarbonate (620 mg, 7.36 mmol) and $(CF_3SO_2)_2O$ (0.68 mL, 4.1 mmol). The resulting mixture was stirred for 15 min. The reaction mixture was warmed to 25 °C and stirring continued for 18 h. The reaction was quenched with H_2O (100 mL) and the resulting solution diluted with EtOAc (200 mL) followed by washing with brine (100 mL), dried ($MgSO_4$), and concentrated by rotary evaporation to give a cream solid that was purified via silica gel chromatography (hexane–EtOAc, 70:30) to give 1,4-bis(4-trifluoromethyl-

sulfonamidophenoxy) butane, **6**, (774 mg). ^{1}H NMR (360 MHz, DMSO-d_6) δ 11.54 (s, br, 2H, 2×N*H*), 7.15 (d, J = 9.2 Hz, 4H), 6.95 (d, J = 9.2 Hz, 4H), 4.02 (m, 4H, 2×CH_2), 1.84 (m, 4H, 2×CH_2). ^{19}F NMR (376.5 MHz, DMSO) δ 75.75 (s, 6F, 2×CF_3). ^{13}C NMR (600 MHz, DMSO-d_6) δ 157.5, 126.8, 125.9, 118.7, 115.1, 67.4, 25.3. MS-EI m/z 536 [M^+]. HRMS calcd for $C_{18}H_{18}F_6N_2O_6S_2$ [M–H]$^-$ 535.0432, found 535.0410.

Bis(4-trifluoromethylsulfonamidophenyl)-1,4-diisopropylbenzene (7). To a solution of α,α′-bis(4-aminophenyl)-1,4-diisopropylbenzene (1 g, 2.9 mmol) in dry CH_2Cl_2 (10 mL) at 0 °C was added sodium bicarbonate (975 mg, 11.6 mmol) and $(CF_3SO_2)_2O$ (0.97 mL, 5.8 mmol). The resulting mixture was stirred for 15 min. The reaction mixture was warmed to 25 °C and stirring continued for 18 h. The reaction was quenched with H_2O (100 mL) and the resulting solution diluted with EtOAc (200 mL) followed by washing with brine (100 mL), dried ($MgSO_4$), and concentrated by rotary evaporation to give a cream solid that was purified via silica gel chromatography (hexane–EtOAc, 70:30) to give bis(4-trifluoromethylsulfonamidophenyl)-1,4-diisopropylbenzene, **7**, (863 mg). ^{1}H NMR (300 MHz, DMSO-d_6) δ 7.18 (m, 4H), 7.07 (m, 8H), 1.57 (s, 12H, 4×CH_3). ^{19}F NMR (376.5 MHz, DMSO) δ-76.08 (s, 6F, 2×CF_3).^{13}C NMR (600 MHz, DMSO-d_6) δ 148.6, 147.1, 132.2, 127.6, 126.1, 122.9, 120.8, 118.6, 39.1, 30.2. MS-EI m/z 608 [M^+]. HRMS calcd for $C_{26}H_{26}F_6N_2O_4S_2$ [M–H]$^-$ 607.1160, found 607.1126.

1,4 - Bis(4 - trifluoromethylsulfonamidophenoxy)benzene (8). To a solution of 1,4-bis(4-aminophenoxy)benzene (500 mg, 1.71 mmol) in dry CH_2Cl_2 (6 mL) at 0 °C was added sodium bicarbonate (575 mg, 6.84 mmol) and $(CF_3SO_2)_2O$ (0.63 mL, 3.7 mmol). The resulting mixture was stirred for 15 min. The reaction mixture was warmed to 25 °C and stirring continued for 18 h. The reaction was quenched with H_2O (100 mL) and the resulting solution diluted with EtOAc (200 mL) followed by washing with brine (100 mL), dried ($MgSO_4$), and concentrated by rotary evaporation to give a cream solid that was purified via silica gel chromatography (hexane–EtOAc, 70:30) to give 1,4-bis(4-trifluoromethylsulfonamidophenoxy) benzene, **8**, (713 mg). ^{1}H NMR (300 MHz, DMSO-d_6) δ 11.7 (s, br, 2H, 2×N*H*), 7.24 (m, 4H), 7.08 (s, 4H), 7.03 (m, 4H). ^{19}F NMR (376.5 MHz, DMSO) δ −75.88 (s, 6F, 2×CF_3). ^{13}C NMR (600 MHz, DMSO-d_6) δ 156.5, 152.8, 130.3, 126.3, 121.5, 119.4, 119.3. MS-EI m/z 556 [M^+]. HRMS calcd for $C_{20}H_{14}F_6N_2O_6S_2$ [M–H]$^-$ 555.0119, found 555.0156.

1,3-Bis(4-trifluoromethylsulfonamidophenoxy)benzene (9). To a solution of 1,3-bis(4-aminophenoxy)benzene (500 mg, 1.7 mmol) in dry CH_2Cl_2 (6 mL) at 0 °C was added sodium bicarbonate (570 mg, 6.84 mmol) and $(CF_3SO_2)_2O$ (0.57 mL, 3.42 mmol). The resulting mixture was stirred for 15 min. The reaction mixture was warmed to 25C and stirring continued for 18 h. The reaction was quenched with H_2O (100 mL) and the resulting solution diluted with EtOAc (200 mL) followed by washing with brine (100 mL), dried ($MgSO_4$), and concentrated by rotary evaporation to give a cream solid that was purified via silica gel chromatography (hexane–EtOAc, 70:30) to give 1,3-bis(4-trifluoromethylsulfonamidophenoxy) benzene, **9**, (689 mg). ^{1}H NMR (360 MHz, DMSO-d_6) δ 11.71 (br s, 2H, 2×N*H*), 7.38 (t, J = 8.2 Hz, 1H), 7.26 (m, 4H), 7.08 (m, 4H), 6.77 (dd, J = 2.2 and 8.2 Hz, 2H), 6.64 (t, J = 2.2 Hz, 1H). ^{19}F NMR (376.5 MHz, DMSO) δ-75.93 (s, 6F, 2×CF_3). ^{13}C NMR (600 MHz, DMSO-d_6) δ 157.8, 154.5, 131.3, 125.3, 120.8, 119.7, 113.5, 108.9. MS-EI m/z 556 [M^+]. HRMS calcd for $C_{20}H_{14}F_6N_2O_6S_2$ [M–H]$^-$ 555.0119, found 555.0164.

3,5-Bis-(4-trifluoromethanesulfonyl-phenoxy)-benzoic acid (10). To a solution of methyl 3,5-dihydroxybenzoate (100 mg, 0.59 mmol) in DMF (9 mL) was added potassium carbonate (330 mg, 2.37 mmol) and 4-(trifluoromethylsulfonyl)chlorobenzene (291 mg, 1.18 mmol). The resulting mixture was heated to 125 °C for 18 h. The reaction was quenched with H_2O (100 mL) and the resulting solution diluted with EtOAc (200 mL) followed by washing with brine (100 mL), dried ($MgSO_4$), and concentrated by rotary evaporation to give 3,5-bis-(4-trifluoromethanesulfonyl-phenoxy)-benzoic acid methyl ester as a cream solid. To a THF:water (1:1, 20 mL) solution of crude 3,5-bis-(4-trifluoromethanesulfonyl-phenoxy)-benzoic acid methyl ester at 25 °C was added potassium hydroxide (25 mg, 0.45 mmol) and stirring for 8 h. The reaction was quenched with 2 M HCl (adjust pH to 4) and the resulting solution diluted with EtOAc (300 mL) followed by washing with brine (100 mL), dried ($MgSO_4$), and concentrated by rotary evaporation to give a cream solid that was purified via silica gel chromatography (CH_2Cl_2–MeOH, 95:5) to give the title compound **10** (201 mg). ^{1}H NMR (300 MHz, DMSO-d_6) δ 8.11 (d, J = 9.2 Hz, 4H), 7.57 (d, J = 2.11 Hz, 2H), 7.39 (d, J = 9.2 Hz, 4H), 7.39 (m, 1H). ^{19}F NMR (376.5 MHz, DMSO) δ −79.13 (s, 6F, 2×CF_3). ^{13}C NMR (600 MHz, DMSO-d_6) δ 165.5, 164.4, 154.9, 133.7, 122.7, 120.5, 118.7, 118.3, 118.2. Anal. calcd for $C_{21}H_{12}F_6O_8S_2$: C, 44.22; H, 2.12. Found: C, 44.67; H, 2.59. HRMS calcd for $C_{21}H_{12}F_6O_8S_2$ [M–H]$^-$ 568.9800, found 568.9853.

4-[3-(4-Trifluoromethanesulfonyl-phenoxy)-phenoxy]-benzoic acid (11). To a solution of 4-(3-hydroxyphenoxy)benzoic acid (100 mg, 0.43 mmol) in DMF (5 mL) was added potassium carbonate (240 mg, 1.74 mmol) and 4-(trifluoromethylsulfonyl)chlorobenzene (106 mg, 0.63 mmol). The resulting mixture was heated to 125 °C for 18 h. The reaction was quenched with 2 M HCl (adjust pH to 4) and the resulting solution diluted with EtOAc (300 mL) followed by washing with brine (100 mL), dried ($MgSO_4$), and concentrated by rotary evaporation to give a cream solid that was purified via silica gel chromatography (CH_2Cl_2–MeOH, 95:5) to give 4-[3-(4-trifluoromethanesulfonyl-phenoxy)-phenoxy]-benzoic acid, **11**, (129 mg). ^{1}H NMR (300 MHz, DMSO-d_6) δ 8.09 (d, J = 8.97 Hz, 2H), 7.95 (d, J = 8.94 Hz, 2H), 7.56 (t, J = 8.54 Hz, 1H), 7.33 (d, J = 8.94 Hz, 2H), 7.10 (d, J = 8.97 Hz, 2H), 7.04–7.11 (m, 3H). ^{19}F NMR (376.5 MHz, DMSO) δ-79.16 (s, 3F, CF_3). ^{13}C

NMR (600 MHz, DMSO-d_6) δ 166.6, 164.6, 160.1, 156.9, 154.8, 133.7, 131.9, 131.6, 125.9, 122.3, 120.5, 118.4, 117.7, 116.9, 112.5. MS-EI m/z 438 [M^+]. HRMS calcd for $C_{20}H_{13}F_3O_6S$ [M–H]$^-$ 437.0307, found 437.0293.

1-(4-Aminophenoxy)-4-trifluoromethylsulfonamidophenoxy benzene (12). To a solution of 1,4-bis(4-aminophenoxy)-benzene (1 g, 3.41 mmol) in dry CH_2Cl_2 (50 mL) at 0 °C was added sodium bicarbonate (1.14 g, 13.6 mmol) and $(CF_3SO_2)_2O$ (0.52 mL, 3.07 mmol). The resulting mixture was stirred for 15 min. The reaction mixture was warmed to 25 °C and stirring continued for 18 h. The reaction was quenched with H_2O (100 mL) and the resulting solution diluted with EtOAc (200 mL) followed by washing with brine (100 mL), dried ($MgSO_4$), and concentrated by rotary evaporation to give a cream solid that was purified via silica gel chromatography (hexane–EtOAc, 70:30) to give 1-(4-aminophenoxy)-4-trifluoromethylsulfonamidophenoxy benzene, **12**, (1.03 g). ^{1}H NMR (300 MHz, DMSO-d_6) δ 7.55 (br s, 2H, NH_2), 7.18 (m, 2H), 6.99 (m, 2H), 6.94 (m, 2H), 6.90 (m, 2H), 6.80 (m, 2H), 6.66 (m, 2H). MS-EI m/z 424 [M^+]. HRMS calcd for $C_{19}H_{15}F_3N_2O_4S$ [M – H]$^-$ 423.0626, found 423.0621.

PTP assays

The following in vitro assay procedures were used to determine the PTP inhibitory activity of the compounds. The catalytic assays were performed in a 96-well format. The general procedure began with the determination of PTP optimal pH using a three-component buffer system that minimizes ionic strength variations across a wide range of buffer pH. Next, the Michaelis–Menten constant, or K_m, was determined for each specific substrate-PTP system. This K_m value was subsequently used as the substrate reaction concentration for compound screening. Finally, the PTP was exposed to varying concentrations of compound for 15 min and allowed to react with the substrate for 10 min. The results were plotted as percentage inhibition versus compound concentration and the IC_{50} interpolated from the plot.

Materials and reagents.

1. Assay buffer was used as solvent for all assay solutions unless otherwise indicated.

Component	Concentration
Acetate (Fisher Scientific A38-500)	100 mM
Bis–tris (Sigma B-7535)	50 mM
Tris (Fisher Scientific BP152-5)	50 mM
Glycerol (Fisher Scientific BP229-1)	10% (v/v)

*1 mM DTT is added immediately prior to use.

2. 96 Well Easy Wash Plate (Costar 3369)
3. *p*-Nitrophenyl phosphate (Boehringer Mannheim 738-379)
4. Fluorescein diphosphate (Molecular Probes F-2999)
5. 0.22 μm Stericup Filtration System 500 mL (Millipore SCGPU05RE)
6. 10N NaOH (Fisher Scientific SS255-1)
7. 10N HCl (Fisher Scientific A144-500)
8. Compounds were dissolved in DMSO (Sigma D-5879) at 5 or 10 mM concentrations and stored at −20 °C in small aliquots.

Methods. All assays were performed using pNPP or FDP as substrate. The optimum pH was determined for each PTP used. PTPase activity was assayed at 25 °C in a 100-μL reaction mixture containing an appropriate concentration of pNPP or FDP as substrate. The reaction was initiated by addition of the PTP and quenched after 10 min by addition of 50 μL of 1 N NaOH. The non-enzymatic hydrolysis of the substrate was corrected by measuring the control without the addition of the enzyme. The amount of *p*-nitrophenol produced was determined from the absorbance at 410 nm. To determine the kinetic parameter, K_m, the initial velocities were measured at various substrate concentrations and the data were fitted to the Michaelis equation where velocity = (V_{max} *[S])/(K_m + [S]), and [S] = substrate reaction concentration.

Inhibition studies. The effect of the compounds on PTP was evaluated at 25 °C using pNPP or FDP as substrate. PTP was pre-incubated for 15 min with various concentrations of compound. Substrate was then added at a fixed concentration (usually equal to the K_m previously calculated). After 10 min, NaOH was added to stop the reaction. The hydrolysis of pNPP was followed at 410 nm on the Biotek Powerwave 200 microplate scanning spectrophotometer. The percentage inhibition was calculated as follows: Percentage inhibition = [(control signal-compound signal)/control signal] × 100%. The IC_{50} was then determined by interpolation of a percentage inhibition versus compound concentration plot.

Plasmids designed for bacterial GST-PTP fusion protein expression were derived by insertion of PCR-generated human PTP fragments into pGEX vectors (Pharmacia Biotech). Several of these constructs were then used to subclone phosphatases into pFastBac-1 for expression in Sf-9 insect cells. Oligonucleotides used for the initial amplification of PTP genes are shown below. The cDNAs were prepared using the Gilbo BRL superscript pre-amplification system on RNAs purchased from Clontech.

PTP SHP-2

SHP-2 cDNA was used as described earlier.[66] The catalytic domain was amplified using the following oligonucleotides:

5′oligo: 5′-TCTGTTGGATCCGAGACACTACAAC-3′ (SEQ ID NO: 2)

3′oligo: 5′-CCGACATCTAGATCAGTCACGATGAA TTCTGCG-3′ (SEQ ID NO: 3)

It was subsequently subcloned into BamH1-Xba-1 sites. It was then ligated into pfas Bac-G2T BamH1-Xba-1 sites.

PTP 1B

The PTP1B cDNA was amplified from human placenta single strand cDNA (Clontech RNA) using the following oligonucleotides:

5′oligo: 5′-CCGACAGGATCCGAGATGGAAAAGGAGTTCGAGCAGATCGAC (SEQ ID NO: 4)

3′oligo: 5′-CCGACATCTAGACTATGTGTTGCTGTTGAACAGGAACCTG (SEQ ID NO: 5)

It was subsequently ligated into pFasBac G2TBam H1Xba-1 sites.

PTP Epsilon

The PTP Epsilon cDNA was amplified from human placenta single-strand cDNA (Clontech RNA) using the following oligonucleotides:

5′oligo: 5′-GCTGGATCCAGCACCAGCGACAAGAAGATG-3′ (SEQ ID NO: 6)

3′oligo: 5′-GTAGTACTCGAGTAAGGCTTGG-3′ (SEQ ID NO: 7)

After cloning this PCR product into the Bam HI/Xho I sites of pGEX 6P-1, this phosphatase was subcloned using the same restriction sites in pFastBac-G2T.

PTP Meg2

The PTP Meg2 cDNA was amplified from human placenta single strand cDNA (Clontech RNA) using the following oligonucleotides:

5′oligo: 5′-GATGAATTCGATGAGATCATCCTGTTCTC-3′ (SEQ ID NO: 8)

3′oligo: 5′-GTACTCGAGTTACTGACTCTCCACGGC-3′ (SEQ ID NO: 9)

It was subsequently ligated into pGex 6P-1 Eco RI/Xho I sites.

PTP Sigma

The PTP Sigma cDNA was amplified from human brain single strand cDNA (Clontech RNA) using the following oligonucleotides:

5′oligo: 5′-TCAGAATTCCGCACCAAATGCCTCCTG-3′ (SEQ ID NO: 12)

3′oligo: 5′-GGCCTCGAGGCTGCGTGCGGGCACTTC-3′ (SEQ ID NO: 13)

It was subsequently ligated into pGex 6P-1 Eco RI/Xho I sites.

PTP Beta

The PTP Beta cDNA used has been described earlier.[67] The catalytic domain was amplified using the following oligonucleotides:

5′oligo: 5′-GAGAATCCCCCTCTGCCCGTCTGAGCATTC-3′ (SEQ ID NO: 16)

3′oligo: 5′-TAGCTCGAGTCTCAATGCCTTGAATAGACTGG-3′ (SEQ ID NO: 17)

It was subsequently cloned into the Eco RI/Xho I sites of pGEX 6P-1.

PTP Mu

The PTP Mu cDNA was amplified from a human lung cDNA library (Clontech) using the following oligonucleotides:

5′oligo: 5′-AAAGAATTCACACTGAGCACATCGGTGCC-3′ (SEQ ID NO: 18)

3′oligo: 5′-TTCCTCGAGAATCTGGCTTGAGTTTGTCTGTG-3′ (SEQ ID NO: 19)

It was subsequently ligated into the Eco RI/Xho I sites of pGEX 6P-1.

The GST fusion protein constructs in pGEX were transformed into BL-21 bacteria for high level GST fusion protein expression. Overnight cultures were diluted 1:10 in fresh LB amp (100 μg/mL) media and after shaking for 1 h, isopropyl β-D-thiogalactopyranoside (IPTG, 100 μM final concentration) was added. After another 4 h shaking at 37 °C, the cells were lysed in PBS, 1% Triton X-100, 1 mg/mL lysozyme, 10 mg/mL aprotinin/leupeptin by sonication and the supernatants were incubated with glutathione-agarose beads (Pharmacia Biotech) overnight at 40 °C. After three washes in TBS with 1% Triton X-100, the GST fusion proteins were eluted with 5 mM reduced glutathione for 10 min at room temperature.

For GST–PTP expression Sf-9 cells were propagated in supplement Grace's insect medium with 5% fetal bovine serum, 50 IU/mL penicillin (Gibco). 1×106 cells /mL were infected with recombinant baculovirus with a multiplicity of infection of 5 or higher. The cells were then incubated at 27 °C for 3 days, collected, then lysed on ice in Triton Lysis buffer (20 mM Tris–HCl, pH 7.5, 150 mM NaCl, 5 mM EDTA, 10% glycerol, 2 mM phenymethylsulfonyl fluoride, 5 μg/mL leupeptin, 2.5 μg/mL aprotinin) for 60 min. After centrifugation, the supernatant was purified on glutathione-agarose beads (Pharmacia Biotech) as described above.

Acknowledgements

We gratefully acknowledge Zhaoyang Wen for the preparation of some of the compounds, John Biltz for the

biochemical screening and kinetic study, Dr. Joe Even for coordinating the project, Dr. Heather Zhang, Dr. Jiu-Xiang Ni, and Weisheng Liang in the chemistry group for the analytical studies of the compounds, Dr. Fan Xiang, Y. Diana Liu, and Yi Yang in the proteomics group for HRMS analyses of the compounds.

References and Notes

1. Fischer, E. H.; Charbonneau, H.; Tonks, N. K. *Science* **1991**, *253*, 401.
2. Denu, J. M.; Dixon, J. E. *Curr. Opin. Chem. Biol.* **1998**, *2*, 633.
3. Hunter, T. *Philos. Trans. R. Soc. Lond. B Biol. Sci.* **1998**, *353*, 583.
4. Zhang, Z. Y. *Cri. Rev. Biochem. Mol. Biol.* **1998**, *33*, 1.
5. Tonks, N. K.; Neel, B. G. *Cell* **1996**, *87*, 365.
6. Elchebly, M.; Payette, P.; Michaliszyn, E.; Cromlish, W.; Collins, S.; Loy, A. L.; Normandin, D.; Cheng, A.; Himms-Hagen, J.; Chan, C. C.; Ramachandran, C.; Gresser, M. J.; Tremblay, M. L.; Kennedy, B. P. *Science* **1999**, *283*, 1544.
7. Barford, D.; Flint, A. J.; Tonks, N. K. *Science* **1994**, *363*, 1397.
8. Jia, Z.; Barford, D.; Flint, A. J.; Tonks, N. K. *Science* **1995**, *268*, 1754.
9. Burke, T. R.; Ye, B.; Yan, X.; Wang, S.; Jia, Z.; Chen, L.; Zhang, Z. Y.; Barford, D. *Biochemistry* **1996**, *35*, 15989.
10. Puius, Y. A.; Zhao, Y.; Sullivan, M.; Lawrence, D. S.; Almo, S. C.; Zhang, Z. Y. *Proc. Natl. Acad. Sci. U.S.A.* **1997**, *94*, 13420.
11. Groves, M. R.; Yao, Z. J.; Roller, P. P.; Burke, T. R.; Barford, D. *Biochemistry* **1998**, *37*, 17773.
12. Pannifer, A. D.; Flint, A. J.; Tonks, N. K.; Barford, D. *J. Biol. Chem.* **1998**, *273*, 10454.
13. Andersen, H. S.; Iversen, L. F.; Jeppesen, C. B.; Branner, S.; Norris, K.; Rasmussen, H. B.; Moller, K. B.; Moller, N. P. H. *J. Biol. Chem.* **2000**, *275*, 7101.
14. Iversen, L. F.; Andersen, H. S.; Branner, S.; Mortensen, S. B.; Peters, G. H.; Norris, K.; Olsen, O. H.; Jeppesen, C. B.; Lundt, B. F.; Ripka, W.; Moller, K. B.; Moller, N. P. H. *J. Biol. Chem.* **2000**, *275*, 10300.
15. Salmeen, A.; Andersen, J. N.; Myers, M. P.; Tonks, N. K.; Barford, D. *Mol. Cell* **2000**, *6*, 1401.
16. Sarmiento, M.; Puius, Y. A.; Vetter, S. W.; Keng, Y. F.; Wu, L.; Zhao, Y.; Lawrence, D. S.; Almo, S. C.; Zhang, Z. Y. *Biochemistry* **2000**, *39*, 8171.
17. Stuckey, J. A.; Schubert, H. L.; Fauman, E. B.; Zhang, Z. Y.; Dixon, J. E.; Saper, M. A. *Nature* **1994**, *370*, 571.
18. Schubert, H. L.; Fauman, E. B.; Stuckey, J. A.; Dixon, J. E.; Saper, M. A. *Protein Sci.* **1995**, *4*, 1904.
19. Fauman, E. B.; Yuvaniyama, C.; Schubert, H. L.; Stuckey, J. A.; Saper, M. A. *J. Biol. Chem.* **1996**, *271*, 18780.
20. Bilwes, A. M.; Hertog, J.; Hunter, T.; Noel, J. P. *Nature* **1996**, *382*, 555.
21. Hoffmann, K. M. V.; Tonks, N. K.; Barford, D. *J. Biol. Chem.* **1997**, *272*, 27505.
22. Nam, H. J.; Poy, F.; Krueger, N. X.; Saito, H.; Frederick, C. A. *Cell* **1999**, *97*, 449.
23. Hof, P.; Pluskey, S.; Dhe-Paganon, S.; Eck, M. J.; Shoelson, S. E. *Cell* **1998**, *92*, 441.
24. Yang, J.; Liang, X.; Niu, T.; Meng, W.; Zhao, Z.; Zhou, G. W. *J. Biol. Chem.* **1998**, *273*, 28199.
25. Yuvaniyama, J.; Denu, J. M.; Dixon, J. E.; Saper, M. A. *Science* **1996**, *272*, 1328.
26. Fauman, E. B.; Cogswell, J. P.; Lovejoy, B.; Rocque, W. J.; Holmes, W.; Montana, V. G.; Piwnica-Worms, H.; Rink, M. J.; Saper, M. A. *Cell* **1998**, *93*, 617.
27. Reynolds, R. A.; Yem, A. W.; Wolfe, C. L.; Deibel, M. R.; Chidester, C. G.; Watenpaugh, K. D. *J. Mol. Biol.* **1999**, *293*, 559.
28. Stewart, A. E.; Dowd, S.; Keyse, S. M.; McDonald, N. Q. *Nature Struct. Biol.* **1999**, *6*, 174.
29. Su, X.; Taddei, N.; Stefani, M.; Ramponi, G.; Nordlund, P. *Nature* **1994**, *370*, 575.
30. Zhang, M.; Van Etten, R. L.; Stauffacher, C. V. *Biochemistry* **1994**, *33*, 11097.
31. Zhang, M.; Zhou, M.; Van Etten, R. L.; Stauffacher, C. V. *Biochemistry* **1997**, *36*, 15.
32. Zhang, M.; Stauffacher, C. V.; Lin, D.; Van Etten, R. L. *J. Biol. Chem.* **1998**, *273*, 21714.
33. Tabernero, L.; Evans, B. N.; Tishmack, P. A.; Van Etten, R. L.; Stauffacher, C. V. *Biochemistry* **1999**, *38*, 11651.
34. Wang, S.; Tabernero, L.; Zhang, M.; Harms, E.; Van Etten, R. L.; Stauffacher, C. V. *Biochemistry* **2000**, *39*, 1903.
35. Burke, T. R.; Yao, Z. J.; Smyth, M. S.; Ye, B. *Curr. Pharm. Design* **1997**, *3*, 291.
36. Burke, T. R.; Zhang, Z. Y. *Biopolymers* **1998**, *47*, 225.
37. Ripka, W. C. *Annu. Rep. Med. Chem.* **2000**, *35*, 231.
38. Yao, Z. J.; Ye, B.; Wu, X. W.; Wang, S.; Wu, L.; Zhang, Z. Y.; Burke, T. R. *Bioorg. Med. Chem.* **1998**, *6*, 1799.
39. Taylor, S. D.; Kotoris, C. C.; Dinaut, A. N.; Wang, Q.; Ramachandran, C.; Huang, Z. *Bioorg. Med. Chem.* **1998**, *6*, 1457.
40. Desmarais, S.; Friesen, R. W.; Zamboni, R.; Ramachandran, C. *Biochem. J.* **1999**, *337*, 219.
41. Yokomatsu, T.; Murano, T.; Umesue, I.; Soeda, S.; Shimeno, H.; Shibuya, S. *Bioorg. Med. Chem. Lett.* **1999**, *9*, 529.
42. Beers, S. A.; Malloy, E. A.; Wu, W.; Wachter, M. P.; Gunnia, U.; Cavender, D.; Harris, C.; Davis, J.; Brosius, R.; Pellegrino-Gensey, J. L.; Siekierka, J. *Bioorg. Med. Chem.* **1997**, *5*, 2203.
43. Ibrahimi, O. A.; Wu, L.; Zhao, K.; Zhang, Z. Y. *Bioorg. Med. Chem. Lett.* **2000**, *10*, 457.
44. Ye, B.; Burke, T. R. *Tetrahedron. Lett.* **1995**, *36*, 4733.
45. Akamatsu, M.; Ye, B.; Yan, X.; Kole, H. K.; Burke, T. R.; Roller, P. P. *Peptide Chem.* **1995**, 369.
46. Roller, P. P.; Wu, L.; Zhang, Z. Y.; Burke, T. R. *Bioorg. Med. Chem. Lett.* **1998**, *8*, 2149.
47. Burke, T. R.; Yao, Z. J.; Zhao, H.; Milne, G. W. A.; Wu, L.; Zhang, Z. Y.; Voigt, J. H. *Tetrahedron* **1998**, *54*, 9981.
48. Pellegrini, M. C.; Liang, H.; Mandiyan, S.; Wang, K.; Yuryev, A.; Vlattas, I.; Sytwu, T.; Li, Y.; Wennogle, L. P. *Biochem.* **1998**, *37*, 15598.
49. Kotoris, C.; Chen, M.; Taylor, S. *Bioorg. Med. Chem. Lett.* **1998**, *8*, 3275.
50. Desmarais, S. D.; Jia, Z.; Ramachandran, C. *Arch. Biochem. Biophys.* **1998**, *354*, 225.
51. Moran, E. J.; Sarshar, S.; Cargill, J. F.; Shahbaz, M. M.; Lio, A.; Mjalli, A. M.; Armstrong, R. W. *J. Am. Chem. Soc.* **1995**, *117*, 10787.
52. Rice, R. L.; Rusnak, J. M.; Yokokawa, F.; Yokokawa, S.; Messner, D. J.; Boynton, A. L.; Wipf, P.; Lazo, J. S. *Biochemistry* **1997**, *36*, 15965.
53. Taing, M.; Keng, Y. F.; Shen, K.; Wu, L.; Lawrence, D. S.; Zhang, Z. Y. *Biochemistry* **1999**, *38*, 3793.
54. Wrobel, J.; Sredy, J.; Moxham, C.; Dietrich, A.; Li, Z.; Sawicki, D. R.; Seestaller, L.; Wu, L.; Katz, A.; Sullivan, D.; Tio, C.; Zhang, Z. Y. *J. Med. Chem.* **1999**, *42*, 3199.
55. Malamas, M. S.; Sredy, J.; Gunawan, I.; Mihan, B.; Sawicki, D. R.; Seestaller, L.; Sullivan, D.; Flam, B. R. *J. Med. Chem.* **2000**, *43*, 995.
56. Malamas, M. S.; Sredy, J.; Moxham, C.; Katz, A.; Xu, W.; McDevitt, R.; Adebayo, F. O.; Sawicki, D. R.; Seestaller, L.; Sullivan, D.; Taylor, J. R. *J. Med. Chem.* **2000**, *43*, 1293.
57. Urbanek, R. A.; Suchard, S. J.; Steelman, G. B.; Knappenberger, K. S.; Sygowski, L. A.; Veale, C. A.; Chapdelaine, M. J. *J. Med. Chem.* **2001**, *44*, 1777.

58. Sarmiento, M.; Wu, L.; Keng, Y. F.; Song, L.; Luo, Z.; Huang, Z.; Wu, G. Z.; Yuan, A. K.; Zhang, Z. Y. *J. Med. Chem.* **2000**, *43*, 146.
59. Insight II 97.0, Molecular Simulations Inc., 9685 Scranton Rd., San Diego, CA 92121.
60. Sybyl 6.4, Tripos Inc., 1699 South Hanley Rd., St Louis, MO 63144.
61. Chen, L.; Wu, L.; Otaka, A.; Smyth, M. S.; Roller, P. P.; Burke, T. R.; Hertog, J.; Zhang, Z. Y. *Biochem. Biophys. Res. Comm.* **1995**, *216*, 976.
62. Zhang, Z. Y.; Maclean, D.; McNamara, D. J.; Sawyer, T. K.; Dixon, J. E. *Biochemistry* **1994**, *33*, 2285.
63. Available Chemicals Directory, MDL Information Systems, Inc., 14600 Catalina St., San Leandro, CA 94577.
64. Catalyst 4.5, Molecular Simulations Inc., 9685 Scranton Rd., San Diego, CA 92121.
65. Jia, Z.; Ye, Q.; Dinaut, A. N.; Wang, Q.; Waddleton, D.; Payette, P.; Ramachandran, C.; Kennedy, B.; Hum, G.; Taylor, S. D. *J. Med. Chem.* **2001**, *44*, 4584.
66. Vogel, W.; Lammers, R.; Huang, J.; Ullrich, A. *Science* **1993**, *259*, 1611.
67. Levy, J. B.; Canoll, P. D.; Silvennoinen, O.; Barnea, G.; Morse, B.; Honegger, A. M.; Huang, J. T.; Cannizzaro, L. A.; Park, S. H.; Druck, T. *J. Biol. Chem.* **1993**, *268*, 10573.